



JOINT INSTITUTE FOR NUCLEAR RESEARCH
Flerov Laboratory of Nuclear Reactions

FINAL REPORT ON THE INTEREST PROGRAMME

*Production and Spectroscopic Investigation of
New Neutron-Rich Isotopes Near the Neutron
N=126 Shell Closure Using the Multinucleon
Transfer Reactions*

Supervisor:

Dr. Viacheslav Vedeneev

Student:

Lutfi Aditya Hasnowo, Russia
Tomsk Polytechnic University

Participation period:

13 February - 26 March, 2023,
Wave 8

Dubna, 2023

Abstract

The basic method of identifying nuclides in experiments on the synthesis of super heavy nuclei is radiochemistry, which is based on the nature of decay chains ending with known nuclei. Because the half-lives of the majority of super heavy nuclei are quite short (from 100 s to 10 ms), kinematic separators are widely used for super heavy nuclei synthesis, allowing them to be separated with high reliability and efficiency, but they do not measure the core mass. The FLNR JINR (Dubna, Russia) developed the MASHA mass spectrometer to measure the mass of super heavy nuclei and investigate their decay or spontaneous fission. The MASHA setting combines ISOL radioactive nuclei synthesis and separation methods with classical mass analysis methods, allowing identification of nuclide masses synthesized over a wide mass range. In this project, α decay core analysis on a mass separator focal plane detector of three reactions ($^{40}\text{Ar} + ^{148}\text{Sm}$, $^{40}\text{Ar} + ^{166}\text{Er}$ and $^{48}\text{Ca} + ^{242}\text{Pu}$) and peak analysis of the histograms of counts versus energy for the isotopes of Hg and Rn obtained through the above reactions and plot a heat map for the isotopes and calibrate the energy levels were carried out.

I. Introduction

The synthesis of new nuclides has stimulated the development of methods for identifying them using the classical mass spectrometric techniques. In contrast to classical mass spectrometry, the masses of new nuclides must be measured online, that is, directly during their synthesis on accelerated heavy ion beams, in the same way as the well-known ISOL method. The FLNR, JINR designed and manufactured the Mass Analyzer of Super Heavy Atoms (MASHA) for this purpose. The unique potential of the mass analyzer can be attributed to its capabilities of measuring the masses of synthesized superheavy element isotopes and, simultaneously, of detecting their α decays and (or) spontaneous fission [1]

The MASHA setup has been designed as a mass separator with a resolving power of about 1700, which allows bulk identification of superheavy nuclides. The setup applied uses the solid ISOL (Isotope Separation On-Line) method. The work in this project is to analyze real data collected from full fusion reaction experiments of three reactions ($^{40}\text{Ar} + ^{148}\text{Sm}$, $^{40}\text{Ar} + ^{166}\text{Er}$ and $^{48}\text{Ca} + ^{242}\text{Pu}$), where using α decay chains from position sensitive Si detectors. The use of a dedicated hybrid pixel detector TIMEPIX with the MASHA setting for identification of neutron-rich Rn isotopes also exists.

II. MASHA Setup

Figure 1 depicts the MASHA structure. It is made up of a hot catcher, an ion source that operates on the principle of electron cyclotron resonance (ECR), a magneto optical analyzer (D1, D2, D3a, D3b), three quadrupole lenses (Q1, Q2, Q3), two sextupole lenses (S1, S2), and a detection system located in the focal plane of the spectrometer. The mass spectrometer's ion-optical scheme was extensively discussed in. In this section, we describe the above-mentioned separate components of the setup and present measurements of the critical separator characteristics [1].

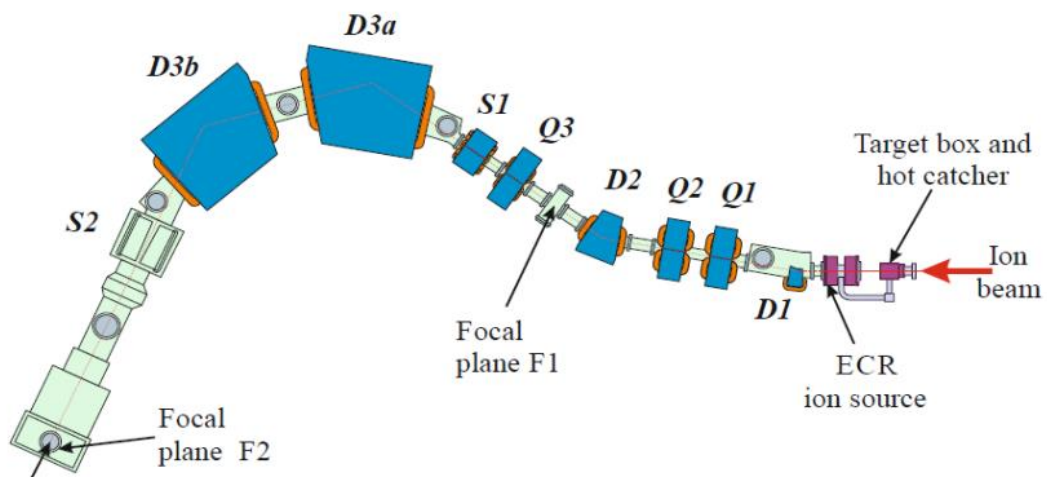


Figure 1. Schematic diagram of the MASHA mass separator: (D1, D2, D3a), and D3b) dipole magnets, (Q1, Q2, Q3) quadrupole lenses, and (S1, S2) sextupole lenses. The detection system is in the focal plane F of the separator

1. Ion Source

Ion Source operates at a very high frequency, in the 2.45 GHz range. The atoms generated by the nuclear fusion reaction are ionized to a charged state of $Q = +1$ and accelerated to 38 keV by a three-electrode electrostatic lens. After that, a magneto-optical mass-to-charge ratio analyzer separates the formed ion beams. The ionization efficiency obtained for the noble gases is about 90%. The ECR ion source is optimized by using noble gases such as Xenon and Krypton, which have the maximum first ionization potential (group VIII of the periodic table) and are chemically inert elements [2].

In **Figure 1**, the operating mode of the ECR source is optimized by selecting the microwave radiation power and frequency, as well as the buffer gas pressure. The MASHA mass separator has dipole magnets (D1, D2, D3a, and D3b), quadrupole lenses (Q1, Q2, Q3), and sextupole lenses (S1, S2). The detection system is located in the focal plane of the F. Ionizer chamber divider. Helium is used as a buffer gas, and a piezoelectric valve is used for pressure regulation and control. The best parameters were obtained at pressures between (1-2) 10^{-5} mbar and a microwave oscillator power of 30 W. **Figure 2** illustrates a schematic of the ECR source with a heat-trapping target [2].

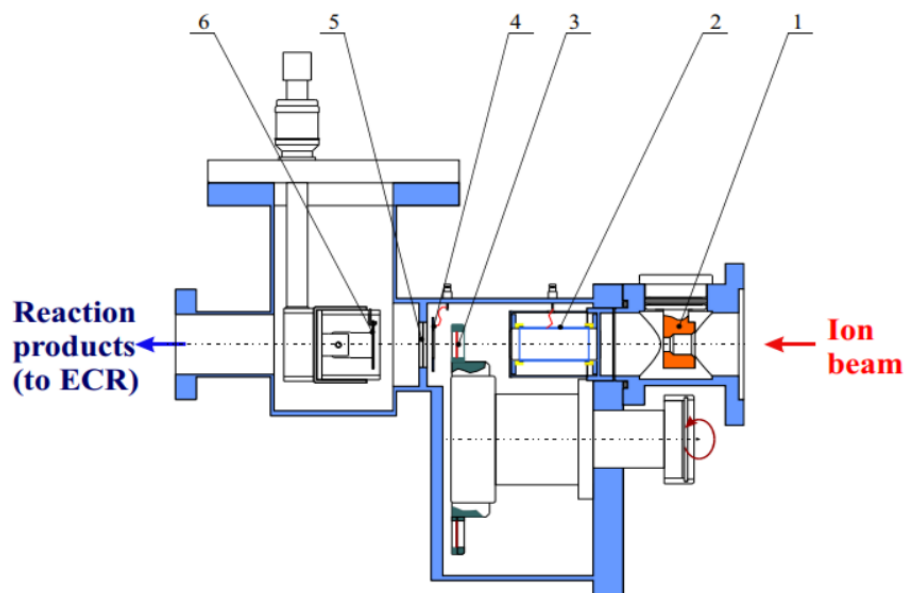


Figure 2. Schematic overview of the target-hot catcher system. Here: (1) diaphragm; (2) pick-up sensor; (3) target on the wheel; (4) electron emission beam monitor; (5) separating foil; (6) hot catcher.

2. Hot catcher and Target Assembly

The product of the fusion reactions is a compound nucleus, which must be "captured" by using a hot catcher that is part of the Target. Figure 3 depicts the entire hot catcher and target scheme. Before reaching the target, the ion beam passes through a diagnostic system comprised of a split aperture, an electrostatic induction sensor, and a Faraday cup. The split aperture is divided into four sectors, each measuring the fraction of the current beam that does not pass through the aperture's hole. The induction sensor, which is essentially a stainless-steel tube mounted on an

electrically isolated frame behind the split aperture, monitors the current during the experiment.

A Faraday cup is placed 70mm in front of the target, which is mounted on a rotational vacuum tight feedthrough. After the fusion reaction occurs following the interaction of the beam with the target, the reaction products exit the target and enter a separating foil, where they are later trapped in a graphite absorber heated to temperatures ranging from 1500 to 2000 K. The products then diffuse as atoms through the pipeline and into the vacuum of the hot catcher. A material made of heated graphite foil with a density of 1g/cm^3 and a thickness of 0.6 mm is used inside the hot catcher. A disc with a diameter of 30mm is placed behind the target, which is made of graphite absorber. A rotating target is used so that heat is distributed uniformly and the target is not damaged. The graphite absorber's temperature is calibrated using an infrared pyrometer. The radiation emitted by the heated graphite was detectable by the pyrometer. The temperature of the graphite absorber was measured during the heater current measurements because the pyrometer could not monitor the temperature during the experiments due to the target assembly configuration [1-3]

3. Detection and Control System

There are many detectors available for detecting nuclear reaction products, such as gas filled tubes (e.g., Geiger Muller) or Scintillator detectors, as well as the most recent of these detectors, semi-conductor detectors. A well-known type of silicon semiconductor detector is used in this work, which is placed in the focal plane of the mass spectrometer. The Frontal detector component is made up of 192 strips that are perpendicular to the direction of the beam and form the detector's frontal sector. The detector is made up of side detectors divided into 16 and 64 strips. **Figure 3** depicts a detector scheme.

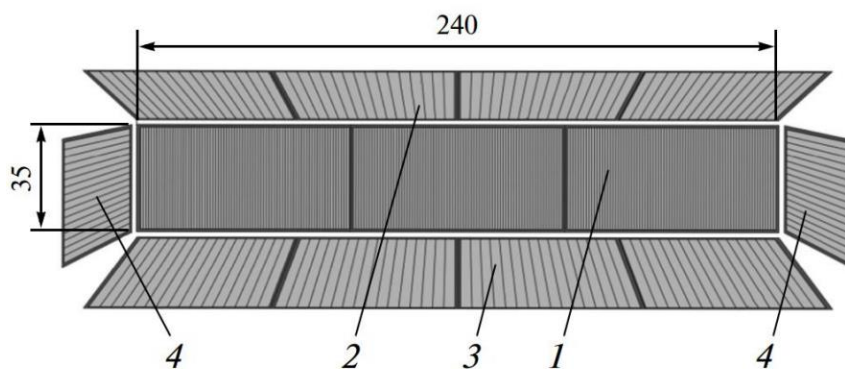


Figure 3. Frontal part (192 strips), (2) top part (64 strips), (3) bottom part (64 strips), and (4) side parts (16 strips in each).

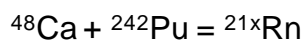
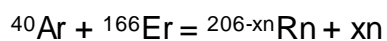
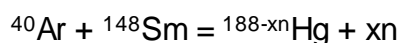
These detectors typically have an operating bias of 40V and an energy resolution of 30keV for particles from a ^{226}Ra source. The detector assembly is designed so that at least 90% of the particles produced by the nuclear reaction are detected in the detector's frontal section. The signals from each detector strip are read out separately. The application makes use of two types of spectra: a one-dimensional spectrum for each strip and a two-dimensional spectrum for each crystal's energy dependence on strip number [3].

4. Data acquisition and beam diagnostics

Upgrading, implementation and testing of new DAQ and beam diagnostics using the highspeed digitizers and high speed digital I/O modules based on PXI and PXIe standards from XIA, Agilent Technologies and National Instruments companies were carried out. The software system for DAQ and beam diagnostics written in C/C++ was also developed and implemented. The silicon strip detector (well type) and TIMEPIX were used in the focal plane of mass-separator MASHA. In case of strip detector, the CAMAC DAQ system was replaced by digitizers. Signals from the silicon strips were recorded via independent spectrometric channels [1].

III. Project Goals

In this project the main goal is performed α decay core analysis on a mass separator focal plane detector of the following reaction:



In addition, to perform peak analysis of the histograms of counts versus energy for the isotopes of Hg and Rn obtained through the above reactions and plot a heat map for the isotopes and calibrate the energy levels.

IV. Method

The method used in the work on the project is to analyze data collected from experiments on full fusion reactions, residual evaporation of neutrons and multinucleon transfer reactions from three reactions $^{40}\text{Ar} + ^{148}\text{Sm}$, $^{40}\text{Ar} + ^{166}\text{Er}$ and $^{48}\text{Ca} + ^{242}\text{Pu}$, using the α decay chain of a position sensitive Si detector. ^{40}Ar and ^{48}Ca extracted

from the U-400M accelerator with energy ~ 7 MeV/nucleon and current up to 0.2 electric μA . The excitation functions were measured with an energy step of ~ 3 MeV. The initial beam energy was measured online by the time of flight method using pickup sensors located at a distance of 1990 mm from each other in the cyclotron channel.

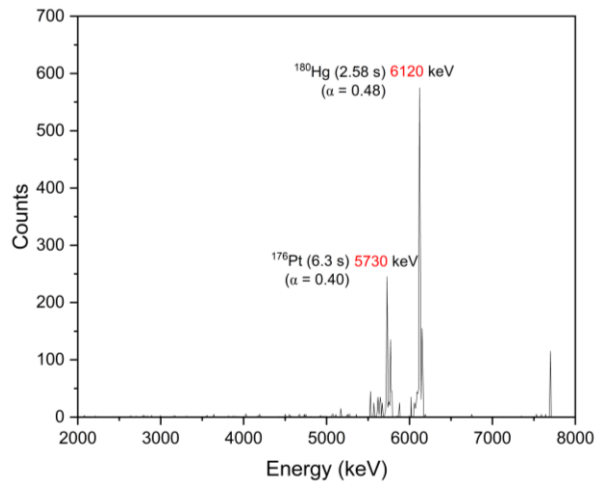
The signals from the pickup sensors were digitized by high speed digitizers. The energy measurement accuracy was 0.5%. By turning the absorber, it was possible to increase its effective thickness and thereby smoothly set the beam energy on the target. The beam later on falls into the graphite absorber where it is stopped. We mentioned that the target assembly consists of a hot catcher, electrostatic induction sensor and a faraday cup, which de facto controls the intensity of the beam. The TIMEPIX custom hybrid pixel detector with the MASHA setting for identification of neutron-rich Rn isotopes was also used in collecting the data. The data obtained is then processed using Origin software to produce histograms of counts versus energy for the isotopes of Hg and Rn obtained through the above reactions and plot a heat map for the isotopes and calibrate the energy levels.

V. Results and Discussion

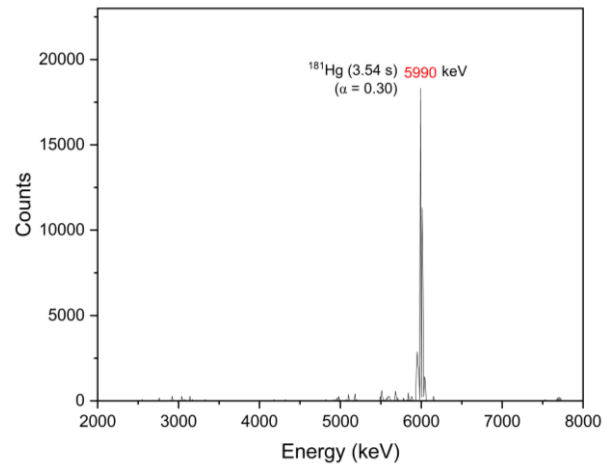
Analysis of the three reactions ($^{40}\text{Ar} + ^{148}\text{Sm}$, $^{40}\text{Ar} + ^{166}\text{Er}$ and $^{48}\text{Ca} + ^{242}\text{Pu}$), where the spectrum of the different isotopes is plotted and further analysed, also heatmaps for the different reactions have been done to visually results.

1. Reactions of $^{40}\text{Ar} + ^{148}\text{Sm} \rightarrow ^{188-x}\text{Hg} + xn$

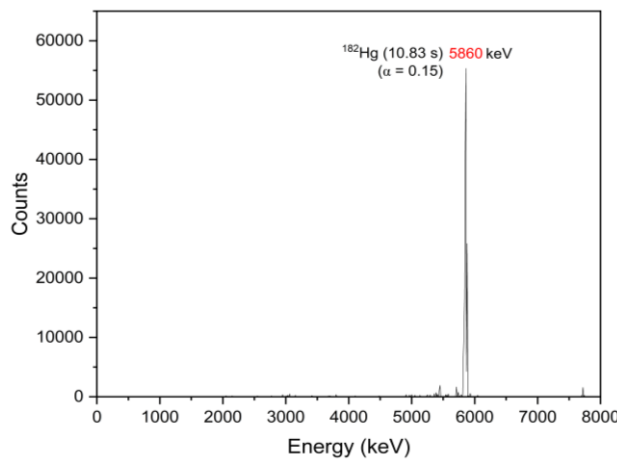
This reaction leads to the production of six isotopes of mercury (^{180}Hg , ^{181}Hg , ^{182}Hg , ^{183}Hg , ^{184}Hg and ^{185}Hg) from which we deduce that the “x” in the reaction formula takes values from 3 to 8, implying that 3 to 8 neutrons “evaporate” during the reaction. These isotopes have been detected through their spectra via their energy releases. **Figure 4** shows the spectra for the different isotopes with their respective peaks in energy and alpha branching ratio for the exact nucleus. There are peaks at different lower energies than the Hg peaks which come from the energy released due to alpha decay of the Hg nucleus and the production of a daughter nucleus which is platinum isotope.



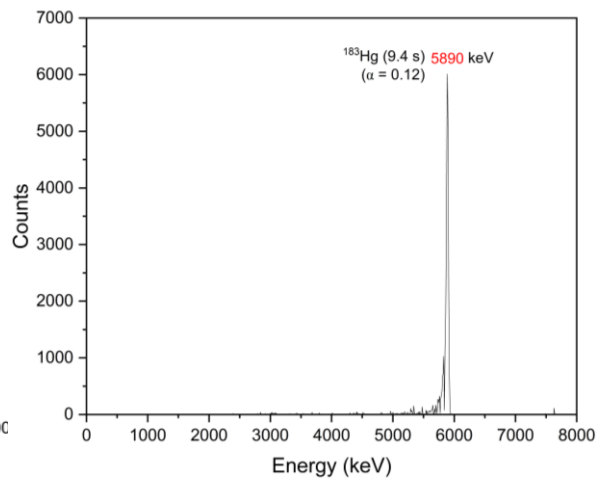
(a)



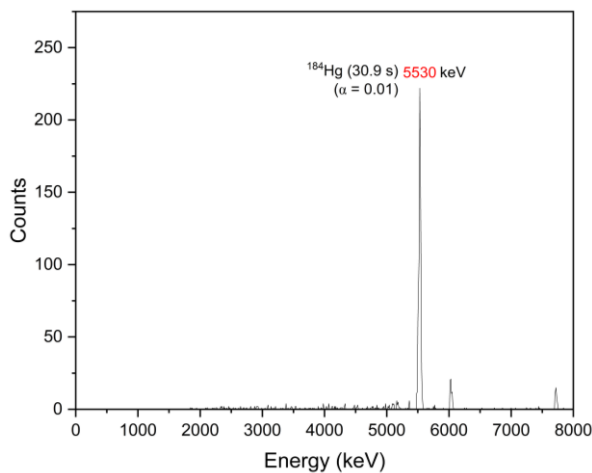
(b)



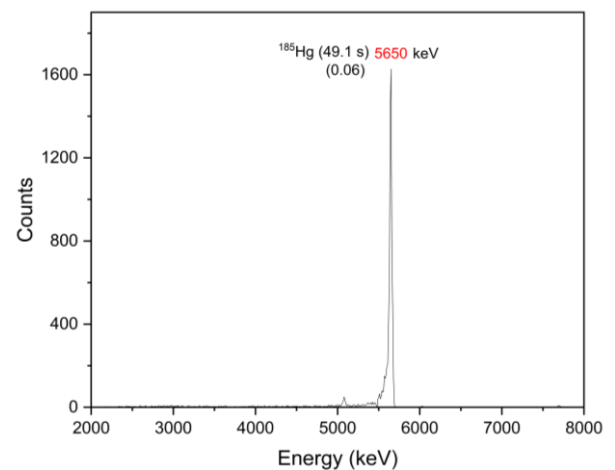
(c)



(d)



(e)



(f)

Figure 4. The energy spectra of mercury isotopes: (a) ^{180}Hg , (b) ^{181}Hg , (c) ^{182}Hg , (d) ^{183}Hg , (e) ^{184}Hg , and (f) ^{185}Hg registered at MASHA setup in the complete fusion reaction $40\text{Ar}+144\text{Sm}$.

Peaks of ^{180}Hg , ^{181}Hg , ^{182}Hg , ^{183}Hg , ^{184}Hg , and ^{185}Hg are identified at energy of 6120 keV, 5990 keV, 5860 keV, 5890 keV, 5530 keV and 5650 keV, respectively.

Figure 4 (a) which shows a peak at 6120 keV representing the energy released from ^{180}Hg , also identified a smaller peak (5730 keV) which represents the energy released by the ^{180}Hg alpha decay product which is ^{176}Pt .

Comparison of radioisotope data obtained from experiments with theoretical data is presented in **Table 1**.

Table 1. Comparison of radioisotope data obtained from experiments and theoretical data

Isotope	$T_{1/2}$	EC or β^+	Alpha	Experimental Energy (KeV)	Theoretical Energy (KeV)	Percentage error
^{180}Hg	2,58 s	0,52	0,48	6120	6119	0,02
^{176}Pt	6,3 s	0,60	0,40	5730	5753	0,40
^{181}Hg	3,54 s	0,70	0,30	5990	6006	0,27
^{182}Hg	10,83 s	0,85	0,15	5860	5867	0,12
^{183}Hg	9,4 s	0,88	0,12	5890	5904	0,24
^{184}Hg	30,9 s	0,99	0,01	5530	5535	0,09
^{185}Hg	49,1 s	0,94	0,06	5650	5653	0,05

The next stage is to present the data matrix or two-dimensional graph where on the X axis is the number of detector strips (separate core positions) while on the Y axis is the energy level of alpha decay. At this stage, the data obtained from the multiplexer/digitizer information is data whose energy level has not been calibrated, so it is necessary to calibrate using data from the one-dimensional histogram of the energy spectra of each isotope. **Figure 5** demonstrates a two-dimensional graph of radon isotopes measured at the focal plane F2 of the facility in the reaction $^{40}\text{Ar} + ^{148}\text{Sm}$ in the middle of the target. This is a two-dimensional graph, where on the X axis are the number of detector strips (positions of separated nuclei), while on the Y axis are the energy levels of alpha decay.

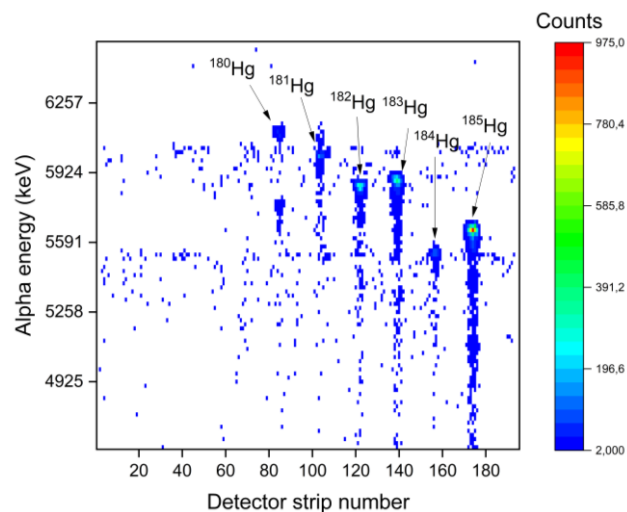
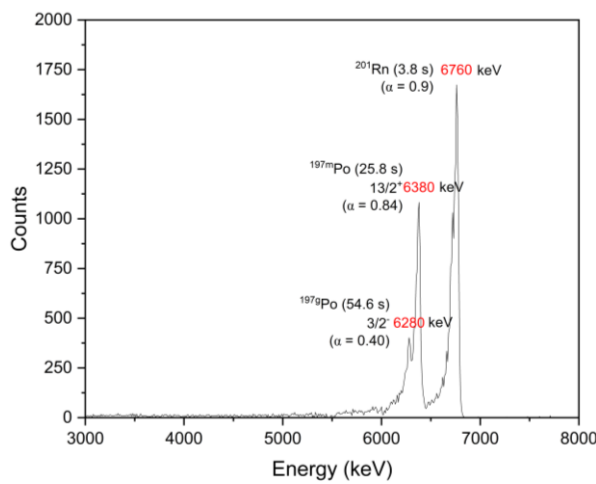


Figure 5. Radon isotopes measured at the focal plane F2 of the facility in the reaction $^{40}\text{Ar} + ^{148}\text{Sm}$

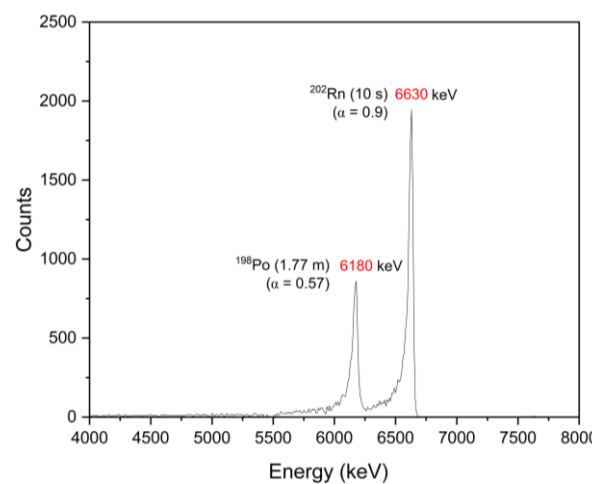
2. Reactions of $^{40}\text{Ar} + ^{166}\text{Er} = ^{206-x}\text{Rn} + x\text{n}$

$^{40}\text{Ar} + ^{166}\text{Er}$ reaction produces five isotopes of Radon: ^{201}Rn , ^{202}Rn , ^{203}Rn , ^{204}Rn and ^{205}Rn . **Figure 6** shows the spectra of the different radon isotopes. Apart from that, another peak has been identified represents the energy released by Polonium (Po) which itself is a product of Radon alpha decay. In spectra 3, apart from the ^{205}Rn peak, another representative peak is also visible the isotope Astatine-205 which is produced by the beta decay of Radon.

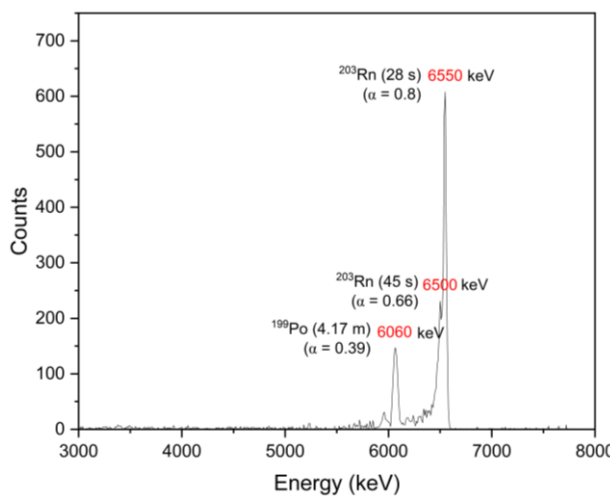
Comparison of radioisotope data obtained from experiments with theoretical data is presented in **Table 2**. **Figure 7** demonstrates radon isotopes measured at the focal plane F2 of the facility in the reaction $^{40}\text{Ar} + ^{166}\text{Er}$ in the middle of the target.



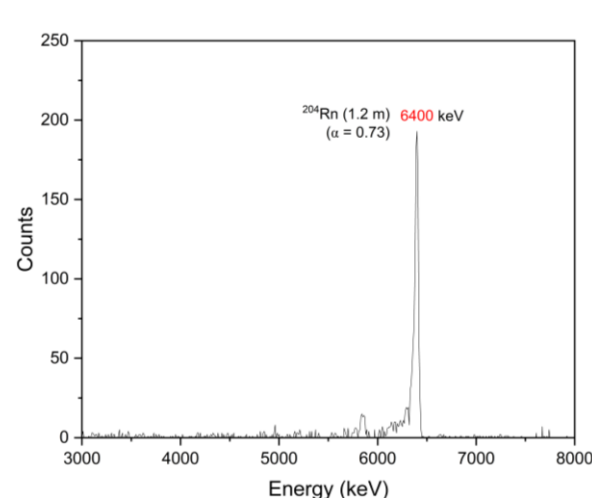
(a)



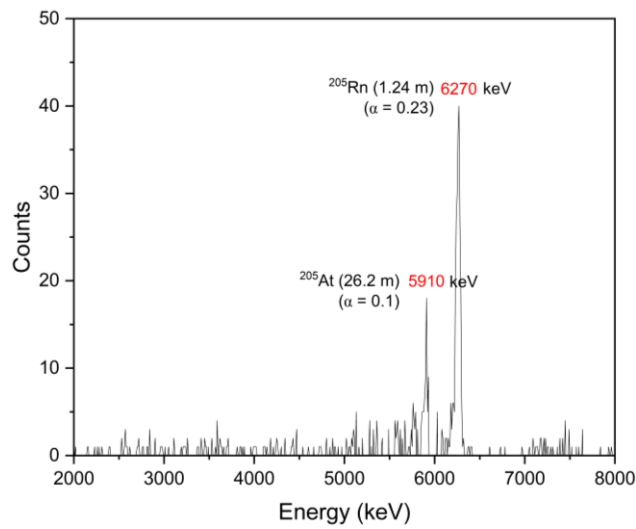
(b)



(c)



(d)



(e)

Figure 6. The energy spectra of mercury isotopes: (a) ²⁰¹Rn, (b) ²⁰²Rn, (c) ²⁰³Rn, (d) ²⁰⁴Rn, and ²⁰⁵Rn registered at MASHA setup in the complete fusion reaction ⁴⁰Ar + ¹⁶⁶Er.

Table 2. Comparison of radioisotope data obtained from experiments and theoretical data

Isotope	T _{1/2}	EC or β ⁺	Alpha	Experimental Energy (KeV)	Theoretical Energy (KeV)	Percentage error
²⁰¹ Rn	7,1 s	0,10	0,9	6760	6725	0,52
^{197m} Po 13/2 ⁺	25,8 s	0,16	0,84	6380	6383,4	0,05
^{197g} Po 3/2 ⁻	53,6 s	0,60	0,40	6280	6281	0,02
²⁰² Rn	10 s	0,10	0,9	6630	6639,5	0,14
¹⁹⁸ Po	1.77 minutes	0,43	0,57	6180	6182	0,03
²⁰³ Rn	28 s	0,20	0,8	6550	6549	0,02
²⁰³ Rn	45 s	0,34	0,66	6500	6499,3	0,01
¹⁹⁹ Po	4.17 minutes	0,61	0,39	6060	6059	0,02
²⁰⁴ Rn	1.2 minutes	0,27	0,73	6400	6418,9	0,29
²⁰⁵ Rn	1.24 minutes	0,77	0,23	6270	6262	0,13
²⁰⁵ At	26.2 minutes	0,90	0,1	5910	5902	0,14

Figure 7. demonstrates a two-dimensional graph of radon isotopes measured at the focal plane F2 of the facility in the reaction ⁴⁰Ar + ¹⁶⁶Er in the middle of the target. This is a two-dimensional graph, where on the X axis are the number of detector strips (positions of separated nuclei), while on the Y axis are the energy levels of alpha decay.

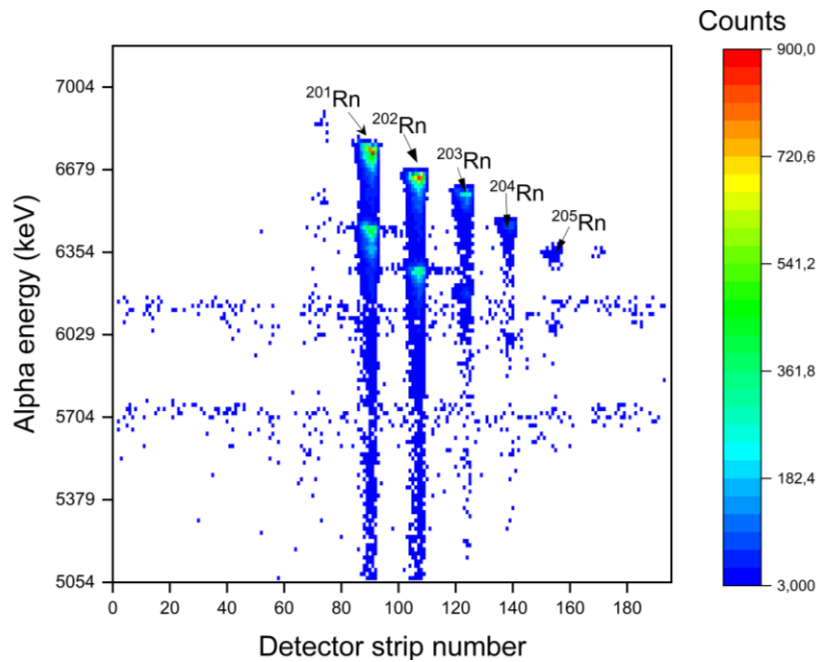


Figure 7. Radon isotopes measured at the focal plane F2 of the facility in the reaction $^{40}\text{Ar} + ^{166}\text{Er}$

3. Reactions of $^{48}\text{Ca} + ^{242}\text{Pu} = ^{21x}\text{Rn}$

The complete energy spectrum of this reaction is presented in **Figure 8**. $^{48}\text{Ca} + ^{242}\text{Pu}$ reaction produces 3 isotopes of radon, namely ^{212}Rn (6250 keV), ^{218}Rn (7110 keV), and ^{219}Rn (6530 and 6600 keV). Alpha decay products from ^{218}Rn were also identified in spectra 5 (b), namely ^{214}Po and ^{210}Po . The energy spectra of the ^{215}Po isotope are also shown in Figure 5(c) as a result of the alpha decay of ^{219}Rn .

Comparison of radioisotope data obtained from experiments and theoretical data for results of $^{48}\text{Ca} + ^{242}\text{Pu} = ^{21x}\text{Rn}$ reaction is presented in **Table 3**. **Figure 9** demonstrates a two-dimensional graph of radon isotopes measured at the focal plane F2 of the facility in the reaction $^{48}\text{Ca} + ^{242}\text{Pu}$ in the middle of the target. This is a two-dimensional graph, where on the X axis are the number of detector strips (positions of separated nuclei), while on the Y axis are the energy levels of alpha decay.

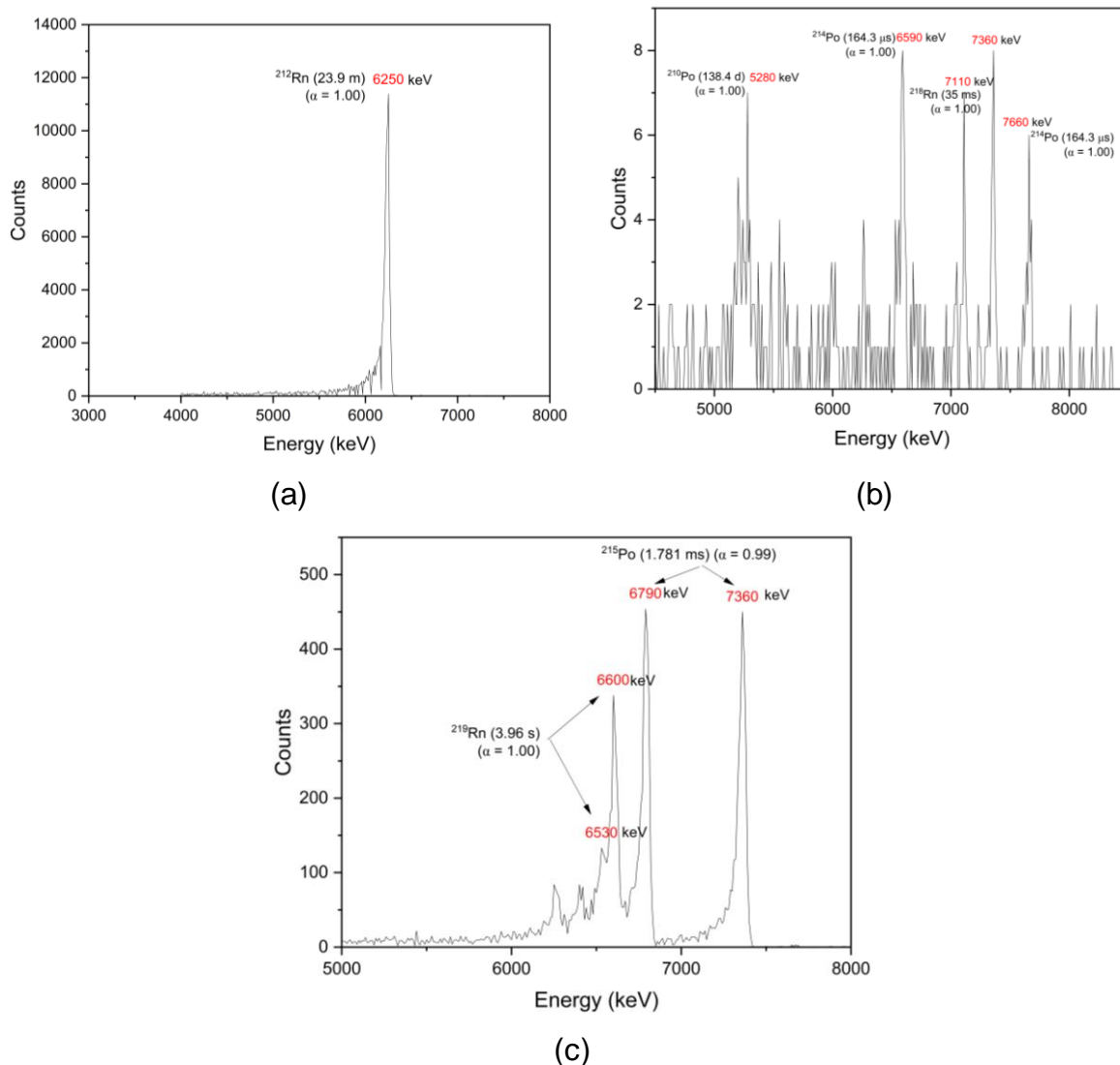


Figure 8. The energy spectra of mercury isotopes: (a) ^{212}Rn , (b) ^{218}Rn , and (c) ^{219}Rn registered at MASHA setup in the complete fusion reaction $^{48}\text{Ca} + ^{242}\text{Pu}$.

Table 3. Comparison of radioisotope data obtained from experiments and theoretical data

Isotope	$T_{1/2}$	EC or β^+	Alpha	Experimental Energy (KeV)	Theoretical Energy (KeV)	Percentage error
^{212}Rn	23.9 minutes	0,00	1	6250	6264	0,22
^{218}Rn	35 ms	0	1	7110	7129,2	0,27
^{214}Po	164.3 μs	0	1	7660	7686,82	0,35
^{214}Po	164.3 μs	0	1	6569	6609,8	0,62
^{210}Po	138.4 d	0	1	5280	5304,33	0,46
^{219}Rn	3.96 s	0	1	6600	6552,6	0,72
^{219}Rn	3.96 s	0	1	6530	6530	0,00
^{215}Po	1.781 ms	0,01	0,99	7360	7386,1	0,35
^{215}Po	1.781 ms	0,01	0,99	6790	6802	0,18

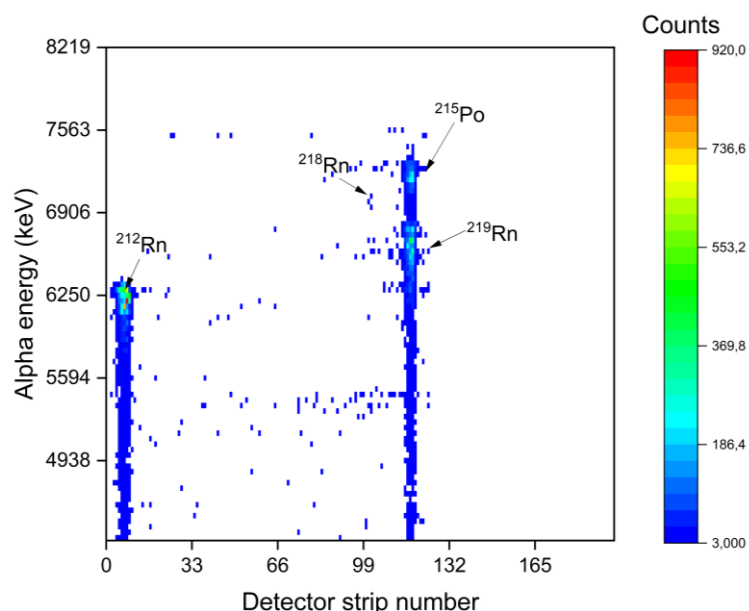


Figure 9. Heat map of radon isotopes measured at the focal plane F2 of the facility in the reaction $^{48}\text{Ca} + ^{242}\text{Pu}$.

VI. Conclusion

Mercury isotopes are produced in the complete fusion reaction of $^{40}\text{Ar} + ^{148}\text{Sm}$ and the isotope Radon is generated by the fusion reaction of $^{40}\text{Ar} + ^{166}\text{Er}$ and from $^{48}\text{Ca} + ^{242}\text{Pu}$ fusion evaporation reaction. The products of $^{40}\text{Ar} + ^{148}\text{Sm} = ^{188-x}\text{Hg} + x\text{n}$ reaction are ^{180}Hg , ^{181}Hg , ^{182}Hg , ^{183}Hg , ^{184}Hg and ^{185}Hg . $^{40}\text{Ar} + ^{166}\text{Er} = ^{206-x}\text{Rn} + x\text{n}$ reactions produce ^{201}Rn , ^{202}Rn , ^{203}Rn , ^{204}Rn and ^{205}Rn . Meanwhile, the reactions of $^{48}\text{Ca} + ^{242}\text{Pu} = ^{21x}\text{Rn}$ produce ^{212}Rn , ^{218}Rn and ^{219}Rn . Alpha decay energy values of isotopes and daughter nuclei, experimentally agreed with the theoretically predicted energies which small deviations are obtained. These results indicate that the MASHA + TIMEPIX setup can be a powerful instrument for the investigation of super heavy isotopes that have limited stability and very short lifetimes.

VII. Acknowledgement

I would like to thank the Joint Institute of Nuclear Research and INTEREST Team for granting me the opportunity to work in this project from which I could learn a lot. I also would like to thank my supervisor Dr. Viacheslav Vedenev for his support in the project.

VIII. References

- [1] A. M. Rodin, E. V. Chernysheva, S. N. Dmitriev, A. V. Gulyaev, D. Kamas, J. Kliman, L. Krupa, A. S. Novoselov, Yu. Ts. Oganessian, A. Opíchal, A. V. Podshibyakin, V. S. Salamatin, S. V. Stepantsov, V. Yu. Vedeneev, S. A. Yukhimchuk, "Features of the Solid-State ISOL Method for Fusion Evaporation Reactions Induced by Heavy Ions", *Exotic Nuclei*, pp. 437-443 (2019), https://doi.org/10.1142/9789811209451_0062
- [2] Vedeneev, V.Y., Rodin, A.M., Krupa, L. et al. The current status of the MASHA setup. *Hyperfine Interact* 238, 19 (2017). <https://doi.org/10.1007/s10751-017-1395-9>
- [3] A. Rodin, A. Belozerov, D. Vanin, V. Y. Vedeneyev, A. Gulyaev, A. Gulyaeva, S. Dmitriev, M. Itkis, J. Kliman, N. Kondratiev, et al., "Masha separator on the heavy ion beam for determining masses and nuclear physical properties of isotopes of heavy and superheavy elements," *Instruments and Experimental Techniques*, vol. 57, no. 4, pp. 386–393, 2014
- [4] S. N. Dmitriev, Y. T. Oganessyan, V. K. Utyonkov, S. V. Shishkin, A. V. Yeremin, Y. V. Lobanov, Y. S. Tsyganov, V. I. Chepygin, E. A. Sokol, G. K. Vostokin, et al., "Chemical identification of dubnium as a decay product of element 115 produced in the reaction $48\text{Ca} + 243\text{Am}$," *Mendeleviev Communications*, vol. 15, no. 1, pp. 1–4, 2005.